European Journal of Mechanics B/Fluids 49 (2015) 243–249

Contents lists available at ScienceDirect

European Journal of Mechanics B/Fluids

journal homepage: www.elsevier.com/locate/ejmflu

Aerodynamic forcing characteristics of dry cable galloping at critical Reynolds numbers

N. Nikitas [a,b,*], J.H.G. Macdonald [a]

[a] Department of Civil Engineering, University of Bristol, BS8 1TR, UK

[b] School of Civil Engineering, University of Leeds, LS2 9JT, UK

ARTICLE INFO

Article history:
Received 11 February 2014
Received in revised form
17 July 2014
Accepted 29 September 2014
Available online 16 October 2014

Keywords:
Cable vibrations
Galloping
Critical flow
Reynolds number
Aerodynamic damping

ABSTRACT

This article attempts to highlight characteristics of the aerodynamic forcing on a rigid circular cylinder experiencing dry galloping vibrations. Observations from a series of wind tunnel tests are studied comparatively with the literature on rain–wind cable vibrations and on flow past inclined lifting bodies such as missiles, for drawing similarities. Unsteadiness and spatial variation of the flow, both previously undermined, are significant during the large cylinder motions recorded. Thus, they are here suspected to play a role in triggering unstable behaviour. Instabilities were restricted to specific ranges of cable-wind angles and Reynolds numbers. The transitional features identified refute the view of simple bursting separation bubbles that rhythmically produce lift and suggest that there is a multitude of paths for energetically feeding dry galloping. Finally explanations are provided and a mechanism incorporating unstable features is proposed for future modelling.

1. Introduction

Large vibrations of bridge cable stays have recently attracted much interest. Specifically the so-called rain–wind-induced vibrations [1,2], which are very often observed on inclined cables, have become a matter of controversy. Different approaches have been proposed for explaining the complex fluid–structure interaction that emerges when rivulets develop on the cable surface due to rain. Modelling the rivulet formation and propagation has been a key element for understanding unwanted cable motions. Actually, two main branches have developed for the explanation of the phenomenon; the one assumes that the appearance of a still rivulet, if appropriately positioned, is adequate to transform the circular profile into an unstable section, as in Den Hartog galloping (e.g. [3]). The other suggests that it is primarily the motion of the formed rivulet that is central in developing large response [4,5]. The role of influencing parameters such as the rainfall intensity, the cable inclination angle and roughness and the motion frequencies have been extensively studied and there is confidence in the knowledge of the combination of these contributions leading to dynamic instability.

However, lately there is additionally growing concern over excessive vibrations of inclined cables that occur under dry conditions, exclusively due to wind, and their understanding seems more elusive. These so-called dry galloping events are believed to share common features with their rain–wind counterparts. Matsumoto et al. [3] first expressed the view that the functioning mechanism is the same for dry or rainy conditions, with rivulets contributing only as an amplification factor. Further similarities were discussed by Macdonald and Larose [6]. A dedicated study that attempted to address similarities between the two phenomena [7] was confined to static models and the comparison was limited to the assessment of the static lift that can be produced in different dry configurations. As a matter of fact the exciting force during dry galloping motion, which could be central to a better understanding, has rarely been recorded and analysed [8,9]. This paper describes a series of large-scale wind tunnel tests which capture subtle forcing details of the dry galloping phenomenon. The objective is to present previously unknown characteristics regarding the unsteadiness of the aeroelastic loading. The well known case of an inclined cylinder with an ogive or conical nose, as in missiles [10,11] provide this work with a very relevant precedent. Further connections are sought with rain–wind [4,12,5] and other flow-induced vibration phenomena [13,14], where unsteadiness also seems important.

2. Wind tunnel tests' background

For the purpose of this experimental work an inclined rigid circular cable model replicating the parameters of a real bridge cable stay (e.g. cable diameter $d = 160$ mm, high density polyethylene smooth finish) was tested in the 6 m × 3 m open circuit wind

* Corresponding author at: School of Civil Engineering, University of Leeds, LS2 9JT, UK. Tel.: +44 131 34 30901.
E-mail address: N.Nikitas@leeds.ac.uk.

http://dx.doi.org/10.1016/j.euromechflu.2014.09.005

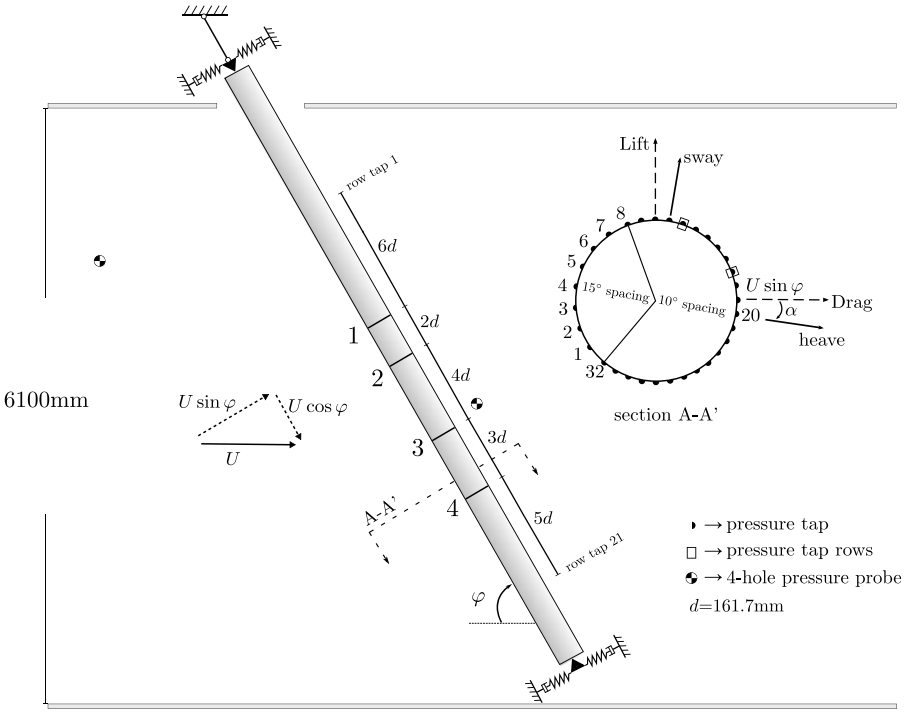

Fig. 1. Elevation of cable model.

tunnel at the National Research Council Canada (NRC). Typical free stream turbulence levels of the wind tunnel are of the order of 0.5%. A detailed illustration of the setup is provided in Fig. 1. More information about the testing was previously given in [8,9]. In short it should be noted that the model could oscillate in two perpendicular planes (denoted sway and heave; see Fig. 1 for the direction convention) and was equipped with pressure measuring taps, arranged at four discrete cross-sections (termed rings) and two axial $21d$-long lines running along the lee side of the cylinder at $1d$ spacings. The support springs could be rotated in order to give different relative orientations of the wind and principal structural axes, considering that the stiffnesses in the two spring planes were not identical (different tuning scenarios were tested but in all cases the frequencies were close to 1.4 Hz). The model could also be locked in place, so as to quantify loads on the stationary cylinder and hence infer the motion-induced aerodynamic effect.

The wind speeds ($U \approx 10$–40 m/s) were selected to span the expected critical Reynolds number range ($\mathrm{Re} \approx [1 - 4.5] \times 10^5$; calculated based on the total mean wind speed vector) and produced large dynamic responses in a number of cases. Interestingly, although a few different inclination and orientation angles were tested ($\varphi = [60°, 77°, 90°]$, $\alpha = [0°, 30°, 55°]$ respectively; both as in Fig. 1), only cables inclined at an angle of 60° to the wind exhibited large responses, mainly across-wind. The largest recorded amplitude was $0.75d$, although this was limited by the support arrangement. Vertical or near vertical configurations of the cable (i.e. $\varphi = 90°$) showed only limited response, while the measured lift and drag forces (for their direction definition see Fig. 1) on the individual pressure rings experienced large sudden jumps, connected with abrupt transitions between different flow states [8]. Specifically, the transition between seemingly subcritical and critical states was observed to occur intermittently on each side of the stationary cylinder even under steady flow conditions. This could be an indication that in these tests there was no strong bias of the flow to give asymmetric lift in one direction or the other. In other similar studies Matteoni and Georgakis [15] and Flamand and Boujard [7] have observed that local lift and drag coefficients were very sensitive to even minute surface alterations, yet it was not possible to determine their global effect along the length. Lamont [11], while testing static ogive-nosed circular cylinders, captured a Reynolds number dependent roll effect (i.e. influence of the orientation α) on force coefficients very consistently. Still, he ascribed this to the asymmetry introduced by the ogive tip, disregarding any possible imperfection of the rest of the nominally axisymmetric cylindrical body.

3. Flow features and excitation mechanism

This section focuses on the pressure distributions that were acquired during large response records. The force evolution is mapped onto an average oscillation cycle and characteristics of the underlying mechanism of the dynamic instability are drawn out. An analytical description of the aeroelastic loading exerted on a cable undergoing dry-galloping vibrations was previously provided through a generalised quasi-steady framework [16,17] encompassing both 3D geometry and Reynolds number effects. In this analysis, valid for small amplitude vibrations the aeroelastic forces are equivalent to pure (negative) viscous damping forces that can possibly overcome the structural damping. However, this straight-forward approach has its limitations and has not been validated. As a matter of fact in other galloping-like phenomena [13,14] a stiffness contribution of the aeroelastic loading was found similarly decisive. The energy input during each vibration cycle is given by integrating over time the product of applied force along the motion direction with velocity. Thus for the current steady-state dry galloping records, with predominantly across-wind character, the local energy input can be assessed by the integral of instantaneous lift on each ring with its velocity. Fig. 2 provides such estimates and clearly indicates that different cable cross-sections contribute different energy inputs to the excitation mechanism, while the energy input over time function remains very linear at all times. Specifically, Ring 3 contributes the most, while Ring 4 extracts energy from the cable (i.e. it acts to damp the response). This finding should not be confused with the observation by Matsumoto et al. [18] of excessive aerodynamic forces on cables being confined to the near-end locations. Ring 3 is

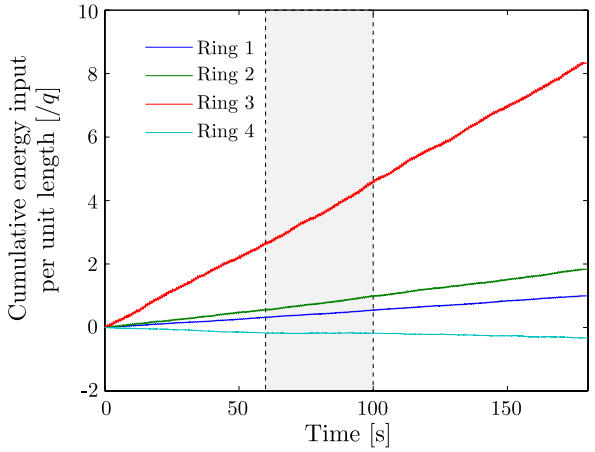

Fig. 2. Scaled energy input during large steady amplitude response ($q = \frac{1}{2}\rho U^2$, where ρ is the air density). Subsequent analysis if not otherwise stated always refers to the grey shaded time interval (i.e. mean cycle interval).

situated centrally and moreover the energy distribution presented in Fig. 2 was specific to the record examined. Other cases (e.g. different wind turbulence, wind speeds or cable angles) produced different results (e.g. Ring 3 damping response and Ring 4 exciting response). These results indicate the complex 3D nature of the flow behaviour and its high sensitivity to the test parameters (Reynolds number, cable inclination angle, etc.). The findings are in line with what was witnessed also by Lamont [11] on an inclined ogive-nosed cylinder. Such bodies exhibit through a wide range of Reynolds numbers high lift values (i.e. force out of the wind–cylinder plane), with a well defined distribution over their length. In transitional regimes though, the regular distribution breaks down with non repeatable lifting patterns emerging.

The actual evolution of the aerodynamic force with motion is further considered. For this purpose a mean cycle is extracted for Ring 3, corresponding to the time interval 60–100 s in Fig. 2. The following discussion and figures, unless otherwise stated, refer to this specific period. Fig. 3 shows the phase-averaged lift force (dashed red line) over the averaged vibration cycle (black lines). Overlayed on these, are polar plots of the pressure coefficient (C_p) distributions, both phase-averaged over the cycle (lines over shaded areas) and averaged over the whole time period (grey dots). Scale-wise the radius of the drawn circles correspond to $C_p = 1$. Evidently the averaged lift force shows clear periodic behaviour related to the motion, but it appears not to be in phase with the velocity. The specific waveforms of the two variables are not identical and the additional higher frequency forcing inputs do not entirely average out. Interestingly the phase lag of the lift with respect to the velocity varies over the cycle. Instants of zero velocity are designated in the figure and the relevant time delays τ_1 and τ_2 to instants of zero lift are evaluated at 1/12 and 1/36 of the vibration period T respectively. Indicatively the characteristic time associated with vortex-shedding $t = d/StU$, where St is the Strouhal number, could range from $T/28$ to $T/65$ depending on the value considered for St (0.2 to 0.48, [19]). For the studied record (i.e. Re $= 3.34 \times 10^5$, $U = 31.5$ m/s) no trace of vortex shedding could be identified. All these features are posing a hurdle for linearised quasi-steady theory, which can only perceive forces as linear products of the motion velocity not allowing naturally for time lags.

Comparing pressure distributions from specific points in the vibration cycle with the overall mean, it is seen that two distinct mechanisms are operating on the different sides of the cylinder. The bottom part presents what seems to be a periodic motion around the cylinder circumference and a change in length of a laminar separation bubble. The quoted separation bubble can be distinguished by the relative flat region that immediately precedes the pressure recovery to the base pressure levels. In Fig. 3 indicative signs were given at 100° from the stagnation point to ease the bubble motion tracking. On the other hand the top seems to alternate between a subcritical-like state (i.e. weak suction on the across-wind pressure taps) to a critical one. However, both parts simultaneously contribute to the forcing throughout the oscillation cycle. Qualitatively the mechanism seems similar to what was put forward for rain–wind vibrations by Verwiebe [4] and Cosentino et al. [5]. According to Verwiebe a single underside rivulet can instigate large motion by causing an early underside separation and thus lift during upward movement. The resulting elliptical motion skews its top part windwards due to the concurrent drag force reduction that follows the lift appearance. This was not the only elliptical behaviour in our tests where also opposite skewness was found depending on test conditions. For Verwiebe's asymmetric excitation mechanism forcing occurs for a limited (and well located time-wise) duration of the vibration cycle, contrary to what is seen in Fig. 3.

The agreement with the Cosentino et al. explanation is more profound. The forcing waveforms are similarly distorted and even the lift-velocity time lag distribution, varying over the vibration period, is much alike. Yet on the other hand this realisation necessitates for a single-sided asymmetry to develop and as was found herein the asymmetry was not necessary for the occurrence of dry-galloping. Cases existed where both cylinder sides were extracting energy from the wind through identical mechanisms. These were mostly cases of two laminar separation bubbles moving as in the bottom cylinder side in Fig. 3, with the main adverse forcing originating from the apparent change in length of each separation bubble. Thus a critical transition and the intermittent formation of a separation bubble is not a necessary condition for instability as was previously thought.

The lift force was further examined to consider the forcing contributions from individual cycles (almost 60 in total). As seen in Fig. 4(a), there is large variation of the forcing over each cycle (black lines) and there are large fluctuations in the forces with time. When their ensemble is considered the result is Fig. 3, and it could be construed that the actual mean effect of the lift force is produced by the local unsteadiness (i.e. jumps). Considering randomly one individual cycle from the ensemble in Fig. 4(b) it is seen that lift coefficient jumps apparently randomly. Yet considering all cycles generally, the largest steps are located close to shortly after $T/4$ and $3T/4$ where the velocity (and the dynamic lift component) changes sign. Such intermittent characteristics seem traceable only possibly through some integrate and fire type model. It is important to note that the time-mean behaviour is much more smooth, setting questions on the statistical interrelations (i.e. cooperation) of jumps between succeeding cycles. Actually the very linear shape over time of the energy input in Fig. 2 is a good indication of the smoothness of the time-mean behaviour.

The energy inputs in Fig. 2 however, are very different implying that the smoothness discussed greatly varies locally between the different rings. Evaluating the average phase lag between lift and displacement over each oscillation cycle for all rings though shows reasonable consistency over three rings. The results are shown in Fig. 5 and strikingly the phase lags for Rings 1–3 are all consistently around a value of 60°. Positive values for the phase lag add energy to the vibration, while negative values extract energy. Ring 4, which acts to damp the motion seems to mainly jump between values around 60°, 0° and −60°, which could be representative of different states for the dry galloping motion. Comparing the results for the four rings, it is notable that the more consistent phase lag (Fig. 5), the greater the mean rate of energy input (Fig. 2).

Considering the spatial distribution of pressures further, data from the axial pressure taps, located at 100° and 150° behind

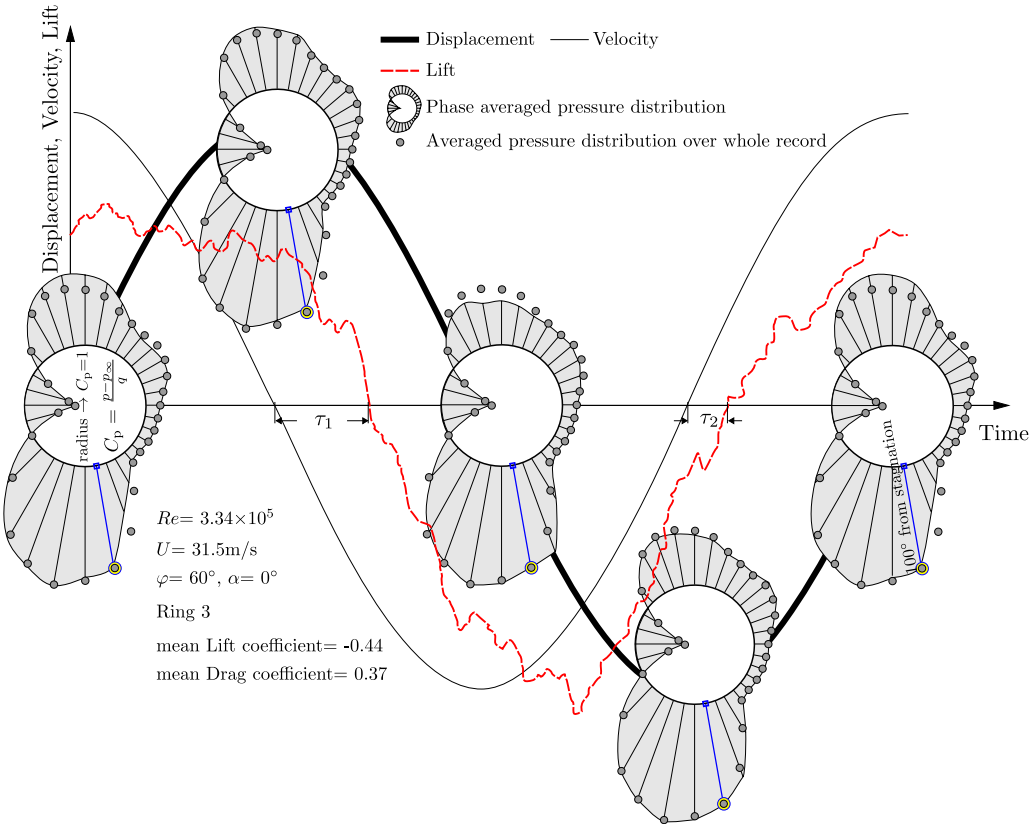

Fig. 3. Averaged sectional aerodynamic forcing through a steady large motion cycle (Ring 3). Indicators are given near the separation point at the underside to track its motion. The time period used corresponds to the shaded area (mean cycle interval) in Fig. 2.

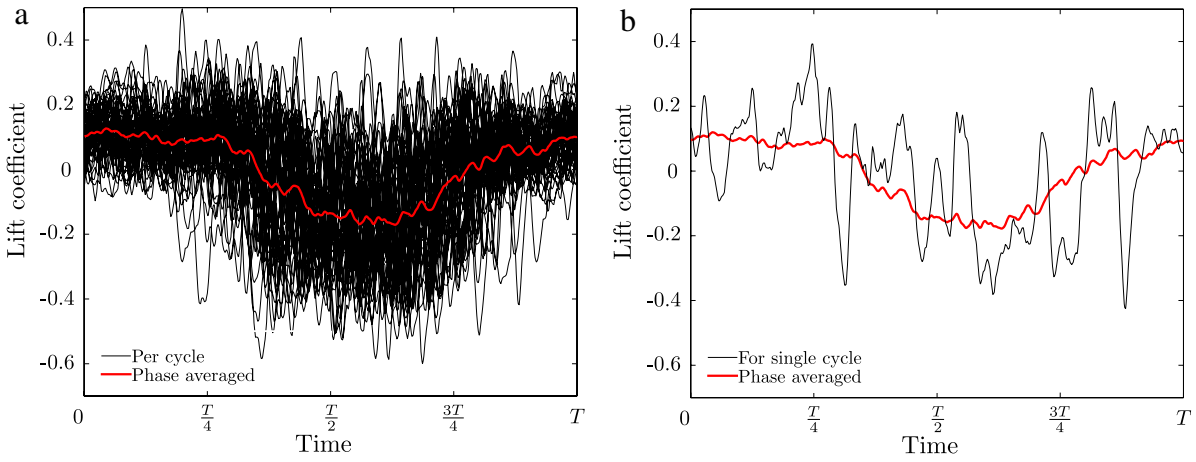

Fig. 4. Lift coefficient for the case illustrated in Fig. 3; (a) Ensemble of the lift variations for each cycle along with their mean, (b) lift variation in one randomly picked cycle alongside the mean of the ensemble.

the stagnation line (Fig. 1), were used to identify the mean pressure profile during oscillation. This is illustrated in Fig. 6. Such information for dynamic models in the transitional Re range is not available in the literature. The relative positions of the two pressure tap lines allow some assessments regarding the state of the flow on the relevant side of the cylinder. At large negative value for pressure coefficients (around −1.5) on taps at 100° from the stagnation point indicate a leeward shift of the separation point, which simplistically implies reattachment of the flow and eventual turbulent separation downstream. Pressure coefficients at 150° from the stagnation point are expected to coincide with the base pressure value, lying distant from the relevant 100° values. The small negative values (around −0.3) along the whole length are a sign that the flow is supercritical, if not necessary on this side of the cylinder definitely on the other. The 100° row pressure taps 17–21 seem to indicate a subcritical state on this side. Along the rest of the length there appears to be fairly regular spacing between positions where transition is not completed and others where it is. Thus it appears that cells may have formed with a characteristic length around 6*d*, with variable separation lines along the length. This is not contradicting with the fast changes recorded in Fig. 2 where sections only 3*d* apart operate in an opposite way. Such cells may consist of a balance between differently operating sections.

Considering the actual pressure distributions of the rings for the studied record there are features that do not fully comply with the

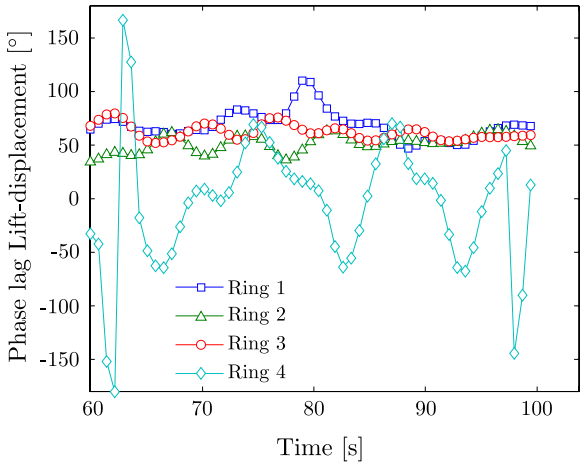

Fig. 5. Phase lag between the lift force and displacement for the mean cycle interval in Fig. 2.

description of the laminar to turbulent transition as this is put forward for non-inclined circular cylinders. In Fig. 7(a) it is seen that Rings 1, 2 and 4 are in very similar post-critical states with separation bubbles having formed unevenly on both sides (near 100° and 250° from the stagnation point respectively). Yet although in terms of mean pressure profiles they are so similar, as far as the dynamic instability is concerned they have opposite functions, with Rings 1 and 2 exciting motion and Ring 4 damping it. Thus it is apparent that the flow state alone is not enough to determine the propensity for dry galloping. Ring 3 on the other hand shows a distinct feature. Its profile is not normal with the plateau near 120° contributing to a sustained asymmetry between the two cylinder sides that protrudes far into the base pressure zone, contrary to classical transitional behaviour. Hence, what was earlier quoted as a subcritical-like state on the top side of the cylinder in Fig. 3 is definitely not just the product of an intermittently bursting laminar separation bubble.

Sectional mean pressure profiles shown from other related cases in the literature, in Fig. 7(b), are used to help understand this behaviour. Cosentino et al. [5] studied rain–wind vibrations of an inclined stay (lower inclination to the one studied herein) and the recorded pressure data on one pressure ring during motion, similarly to this study. For the same conditions they also ran dry tests to address the effect of water on the cylinder surface. Their output in Fig. 7(b) interestingly shows asymmetries alike to those found here that extend into the base pressure region. The values on the other hand are quite different. In particular the minimum suction reaches almost −4, lower than −3 that corresponds to potential flow which is a physical limit for circular cylinders normal to the wind. Yet these limits should not apply to this more complex inclined case where vortex and 3D geometry effects could alter the pressure minimum.

Lamont [11], as previously quoted, worked on static ogive cylinders. He too recorded mean sectional pressures for transitional Reynolds numbers. For conditions close to our study, $\varphi = 55°$ and Re $\approx 4 \times 10^5$, he identified two distinct interesting cases, illustrated in Fig. 7(b). In case 1 the pressure distribution is quantitatively almost identical to the one for Ring 3 in Fig. 7(a). The only difference is that the base pressure region lies on the level of the unforeseen plateau of Ring 3 and is also symmetric. Such profiles according to Lamont were able to produce high lift values, although their repeatability and distribution were unpredictable. Thus all details match our observations well. In a second case Lamont, attempting to identify the effect of axial vortices originating from the expected nose asymmetry and propagating downstream, found what is presented in Fig. 7(b) as case 2. After the early separation at around 80° a secondary vortex produces a second minimum pressure region. There is a great difference between the two sides of the cylinder and it seems there is some similarity with Ring 3 in the current study. Notably the value of the minimum pressure coefficient is again lower than −3, as found by Cosentino et al.. This effect and similar pressure forms disappeared for larger inclinations ($> \sim 70°$). From these comparisons it seems that particular unusual features found during excessive dry galloping vibrations could also be relevant in other cases.

Lamont's tests were preceded by another series of similar tests by Lamont and Hunt [10] where it was shown that long abrupt pressure jumps were locally occurring repeatedly. It was then suspected that this was an effect of turbulence (of the order of 0.5% in the tests) and the subsequent series of tests [11] performed in a lower turbulence wind tunnel (0.05%) were thought to avoid this unstable feature that could make any reference to mean data inaccurate.

For the tests reported here, aerodynamic forcing during large vibrations was seen to be accompanied by erratic behaviour. This could in some respect average out, however the nature of the noise-like behaviour and moreover its time and spatial distribution (e.g. timing of jumps such as those in Fig. 4(b)) are entirely unknown. Although averages can hide unsteady features the contribution of such noise in the underlying mechanism of the dynamic instability could be significant. A different type of jump behaviour was recorded for non-inclined cylinders. The lift force for the dynamic cable model when in low amplitude response (typically below $0.1d$) is presented in Fig. 8. The mean wind speed and Reynolds number is very close to the previously illustrated example, as can be seen in the figure legend. The characteristic

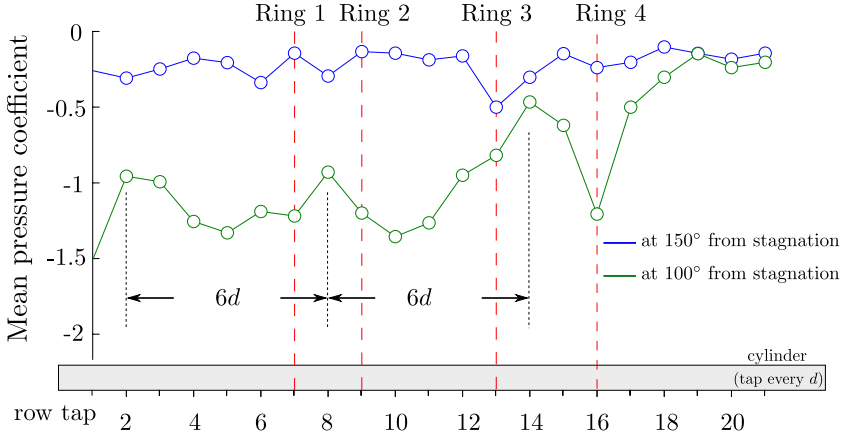

Fig. 6. Pressure distributions along the cable model for the whole record in Fig. 2, indicating patterning.

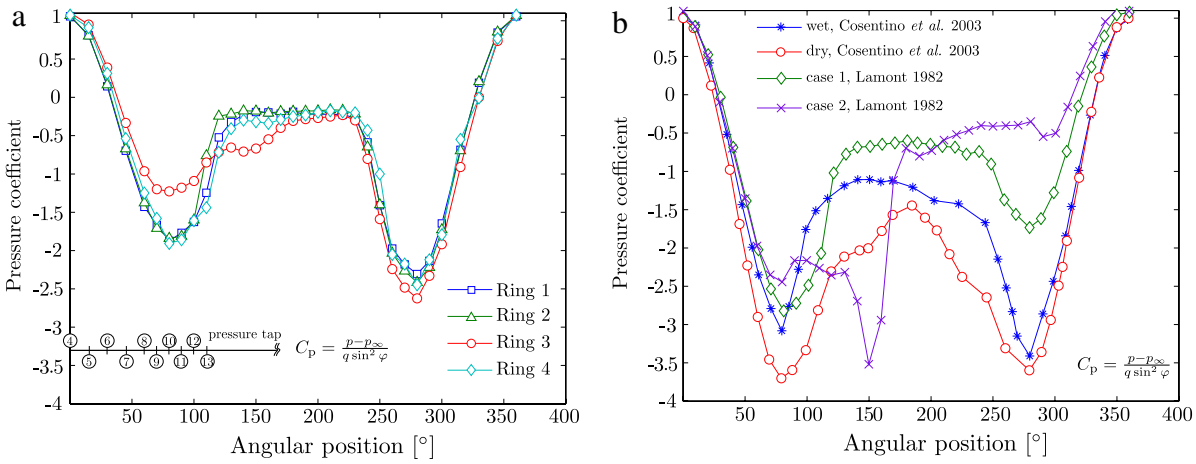

Fig. 7. (a) Mean pressure distributions on all rings for the whole record in Fig. 2, (b) Mean pressure distributions from the literature corresponding to rain–wind vibration and static inclined ogive cylinders.

time of one of this recorded jumps was found to be 0.068 s. This is in good agreement with what was found for a static cylinder by Schewe [19]. For a transition of lift coefficient from 0 to 1 (i.e. double the one in Fig. 8) he got a value of 0.15 s. Strikingly the jumps in the shown case, appear as a succession of rectangular pulses with a regular time spacing between them. This corresponds to a frequency of 4.45 s^{-1} = 0.225 Hz, much lower (almost 1/6th) than the actual motion frequency. Therefore it is questionable whether a vertical cable with frequency close to this value will produce large response owing to some form of ordinary or adaptive resonance loading. Thus, although during testing no vertical (or highly inclined) cable configuration experienced considerable oscillations it seems that they do hold features that potentially could instigate large motion.

4. Concluding remarks

Summarising the main observations presented, it is believed that the effect of transitional behaviour is central for cases of dry galloping. The inherent flow pattern unsteadiness in the critical Re range and its interaction with turbulence and inclination are important in creating the dry galloping conditions. Something similar was also seen for wake-induced vibrations [13,14], where quasi-steady features have to combine with unsteadiness to yield excessive unconventional dynamic response. Abrupt transitions, varying time delays between load and motion, and a stiffness-like wind force component are other characteristics in common between that cases and the current one.

The features of the dry galloping mechanism captured in these tests do not involve simple bursting of a laminar separation bubble. Characteristics related to axial vortices as previously seen in the study of inclined missiles appear to be present in the cable aerodynamic forcing and contribute towards the excitation mechanism. Although significant links were found with rain–wind vibrations it seems that one of the most interesting features is something previously undiscussed even for them and lies in the contribution of noise-like unsteadiness. The current observations suggest that dry galloping is related to some kind of organisation of the noise that arises from both the transitional behaviour and possibly the ambient turbulence. This type of mechanism can be seen to also cooperate with more conventional features, such as a consistent incidence dependence (or else roll effect) that its study seems to be getting growing interest.

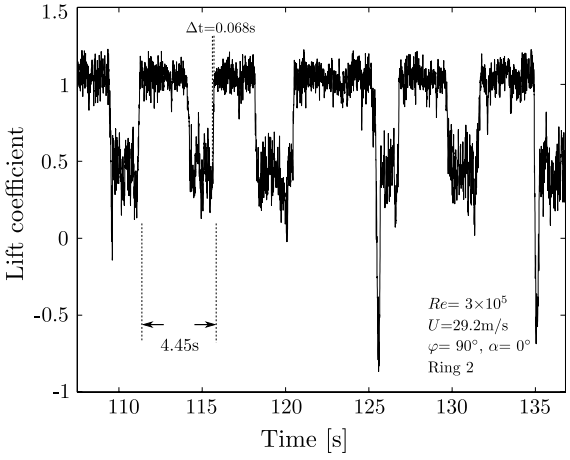

Fig. 8. Unsteady flow transitions during small motion of a non-inclined cylinder.

Acknowledgements

The contributions of Jasna Jakobsen and Terje Andersen (University of Stavanger), Mike Savage, Guy Larose and Brian McAuliffe (NRC) and the technical staff at NRC are gratefully acknowledged. The tests were funded by NRC, EPSRC (via an Advanced Research Fellowship, EP/D073944/1, of the second author), the University of Stavanger and StatoilHydro ASA.

References

[1] M.P. Païdoussis, S.J. Price, E. de Langre, Fluid–Structure Interactions. Cross-Flow-Induced Instabilities, Cambridge University Press, New York, 2011.
[2] E. Caetano, Structural Engineering Documents 9; Cable Vibrations in Cable-Stayed Bridges, IABSE-AIPC-IVBH, Zurich, 2007.
[3] M. Matsumoto, N. Shiraishi, H. Shirato, Rain-wind induced vibration of cables of cable-stayed bridges, J. Wind Eng. Ind. Aerodyn. 43 (1992) 2011–2022.
[4] C. Verwiebe, Exciting mechanisms of rain-wind-induced vibrations, Struct. Eng. Int. 8 (2) (1998) 112–117.
[5] N. Cosentino, O. Flamand, C. Ceccoli, Rain-wind induced vibration of inclined stay cables. Part I: experimental investigation and physical explanation, Wind Struct. 6 (6) (2003) 471–484.
[6] J.H.G. Macdonald, G.L. Larose, Two-degree-of-freedom inclined cable galloping—part 2: analysis and prevention for arbitrary frequency ratio, J. Wind Eng. Ind. Aerodyn. 96 (2008) 308–326.
[7] O. Flamand, O. Boujard, A comparison between dry cylinder galloping and rain-wind induced excitation, in: Proceedings of the 5th European & African Conference on Wind Engineering, EACWE5, Florence, Italy, 2009.
[8] N. Nikitas, J.H.G. Macdonald, J.B. Jakobsen, T.L. Andersen, Critical Reynolds number and galloping instabilities: experiments on circular cylinders, Exp. Fluids 52 (2012) 1295–1306.
[9] J.B. Jakobsen, T.L. Andersen, J.H.G. Macdonald, N. Nikitas, M.G. Savage, B.R. McAuliffe, Wind-induced response and excitation characteristics of an inclined cable in the critical Reynolds number range, J. Wind Eng. Ind. Aerodyn. 110 (2012) 100–112.

[10] P.J. Lamont, B.L. Hunt, Pressures and force distribution on a sharp-nosed circular cylinder at large angles of inclination to a uniform subsonic stream, J. Fluid Mech. 76 (1976) 519–559.
[11] P.J. Lamont, Pressures around an inclined ogive cylinder with laminar, transitional, or turbulent separation, AIAA J. 20 (11) (1982) 1492–1499.
[12] O. Flamand, J.L. Peube, P. Papanikolas, An explanation of the rain-wind induced vibration of inclined stays, in: 4th International Symposium on Cable Dynamics, Montréal, Canada, 2001, pp. 69–76.
[13] G.R.S. Assi, P.W. Bearman, J.R. Meneghini, On the wake-induced vibration of tandem circular cylinders: the vortex interaction excitation mechanism, J. Fluid Mech. 661 (2010) 365–401.
[14] G.R.S. Assi, P.W. Bearman, B.S. Meneghini, J.R. Carmo, S.J. Sherwin, R.H.J. Willden, The role of wake stiffness in the wake-induced vibration of the downstream cylinder of a tandem pair, J. Fluid Mech. 718 (2013) 210–245.
[15] G. Matteoni, C.T. Georgakis, Effects of bridge cable surface roughness and cross-sectional distortion on aerodynamic force coefficients, J. Wind Eng. Ind. Aerodyn. 104–106 (2012) 176–187.
[16] J.H.G. Macdonald, G.L. Larose, A unified approach to aerodynamic damping and drag/lift instabilities, and its application to dry inclined cable galloping, J. Fluids Struct. 22 (2006) 229–252.
[17] J.H.G. Macdonald, G.L. Larose, Two-degree-of-freedom inclined cable galloping—part 1: general formulation and solution for perfectly tuned system, J. Wind Eng. Ind. Aerodyn. 96 (2008) 291–307.
[18] M. Matsumoto, T. Yagi, Y. Shigemura, D. Tsushima, Vortex-induced cable vibration of cable-stayed bridges at higher reduced wind velocity, J. Wind Eng. Ind. Aerodyn. 89 (2001) 633–647.
[19] G. Schewe, Sensitivity of transition phenomena to small perturbation in flow round a circular cylinder, J. Fluid Mech. 172 (1986) 33–46.